ADVANCED ELECTRONIC MATERIALS
www.advelectronicmat.de

Doping High-Mobility Donor–Acceptor Copolymer Semiconductors with an Organic Salt for High-Performance Thermoelectric Materials

Jing Guo, Guodong Li, Heiko Reith, Lang Jiang, Ming Wang, Yuhao Li, Xinhao Wang, Zebing Zeng, Huaizhou Zhao, Xinhui Lu, Gabi Schierning, Kornelius Nielsch, Lei Liao, and Yuanyuan Hu**

Organic semiconductors (OSCs) are attractive for fabrication of thermoelectric devices with low cost, large area, low toxicity, and high flexibility. In order to achieve high-performance organic thermoelectric devices (OTEs), it is essential to develop OSCs with high conductivity (σ), large Seebeck coefficient (S), and low thermal conductivity (κ). It is equally important to explore efficient dopants matching the need of thermoelectric devices. The thermoelectric performance of a high-mobility donor–acceptor (D–A) polymer semiconductor, which is doped by an organic salt, is studied. Both a high p-type electrical conductivity approaching 4 S cm^{-1} and an excellent power factor (PF) of 7 μW K^{-2} m^{-1} are obtained, which are among the highest reported values for polymer semiconductors. Temperature-dependent conductivity, Seebeck coefficient and power factor of the doped materials are systematically investigated. Detailed analysis on the results of thermoelectric measurements has revealed a hopping transport in the materials, which verifies the empirical relationship: $S \propto \sigma^{-1/4}$ and $PF \propto \sigma^{1/2}$. The results demonstrate that D–A copolymer semiconductors with proper combination of dopants have great potential for fabricating high-performance thermoelectric devices.

Energy and environment are still two major issues that are currently widely concerned and urgently need to be solved. It is equally important to reuse waste energy as well as develop new energy sources. For instance, thermoelectric (TE) materials could convert environmental waste heat, such as automobile exhaust and industrial waste heat, burning lost heat and excess solar heat, etc. into electrical energy, which is promising for relieving energy shortages and reducing environmental pollution.[1–3] Excellent thermoelectric materials are supposed to have both good electrical conductivity and poor thermal conductivity, and their performance is ultimately determined by a dimensionless thermoelectric figure of merit, known as ZT:

$$ZT = \frac{S^2 \sigma T}{\kappa} \quad (1)$$

J. Guo, Prof. L. Liao, Prof. Y. Hu
Key Laboratory for Micro/Nano Optoelectronic Devices of Ministry of Education & Hunan Provincial Key Laboratory of Low-Dimensional Structural Physics and Devices
School of Physics and Electronics
Hunan University
Changsha 410082, China
E-mail: yhu@hnu.edu.cn

Prof. G. Li, Prof. H. Zhao
Beijing National Laboratory for Condensed Matter Physics
Institute of Physics
Chinese Academy of Sciences
Beijing 100190, China
E-mail: gdli@iphy.ac.cn

The ORCID identification number(s) for the author(s) of this article can be found under https://doi.org/10.1002/aelm.201900945.

DOI: 10.1002/aelm.201900945

Prof. G. Li, Dr. H. Reith, Dr. G. Schierning, Prof. K. Nielschm
Institute for Metallic Materials
IFW Dresden
Helmholtzstr 20
D-01069 Dresden, Germany

Prof. L. Jiang
Beijing National Laboratory for Molecular Sciences
Key Laboratory of Organic Solids
Institute of Chemistry Chinese Academy of Sciences
Beijing 100190, China

Prof. M. Wang
Center for Advanced Low-Dimension Materials
State Key Laboratory for Modification of Chemical Fibers and Polymer Materials
College of Materials Science and Engineering Donghua University
Shanghai 201620, China

Y. Li, Prof. X. Lu
Department of Physics
The Chinese University of Hong Kong
Shatin 999077, Hong Kong

X. Wang, Prof. Z. Zeng
State Key Laboratory of Chemo/Biosensing and Chemometrics
College of Chemistry and Chemical Engineering
Hunan University
Changsha 410082, China

where T is the absolute temperature (K), S is the thermopower or Seebeck coefficient (V K^{-1}), σ is the electrical conductivity (S m^{-1}), and κ is the thermal conductivity (W K^{-1} m^{-1}). Among these parameters, the product of S^2 and σ is called PF, which is also an important parameter for estimating TE performance.[4–6] A high ZT value is correlated with a high energy conversion efficiency, which means that more energy can be obtained with the same amount of heat. The development of high-efficiency TE devices mainly relies on the development of TE materials owing high ZT values. Presently, the majority macro or micro TE devices are achieved mainly using inorganic semiconductors such as Bi_2Te_3 and its compounds.[7–10] However, these materials are generally toxic, rigid, brittle, and spare, rending them limited applications in some cases.

In contrast, organic semiconductor materials, due to the attractive advantages of light-weight, flexibility, and low-cost processing methods, have become a focus in many research fields over the past few decades, such as organic light-emitting diodes (OLEDs),[11] organic field-effect transistors (OFETs),[12] and organic photovoltaics (OPVs).[13] Organic semiconductors have also gained intensive interest for applications in thermoelectric devices because of their intrinsic low κ values, and great progress has been made in the development of organic thermoelectric devices (OTEs).[5,14–17] The most heavily studied organic material for OTE applications is PEDOT: PSS, which is commonly used in OLEDs and OPVs as a highly conductive polymer, and yields the best thermoelectric performance with a ZT value of 0.42.[18] Poly(2,5-bis(3-dodecylthiophen-2-yl) thieno[3,2-b]thiophene) (PBTTT)[19] and poly 3-hexylthiophene (P3HT)[20] are two p-type organic semiconductors which have been frequently investigated for thermoelectric studies. Due to the low conductivity in pristine organic semiconductors, doping is generally indispensable for achieving high thermoelectric performance. For example, Kemerink et al. have shown sequential "surface doping" by spin–coating organic semiconductor (P3HT) solution and dopant (F_4TCNQ) solution in sequence. A conductivity of 4 S cm^{-1} of and PF around 7 μW K^{-2} m^{-1} were achieved for very thin films (25 nm).[21] Chabinyc et al. reported vapor-doping PBTTT with F_4TCNQ, and obtained a σ of 670 S cm^{-1} and a S of 42 μV K^{-1}, which lead to a large PF of 120 μW K^{-2} m^{-1}.[22] Inspired by the fact that the performance of n-type OTEs is much lagging behind the p-type counterparts, in recent years researchers have paid intensive attention to investigating OTEs based on n-type semiconductors.[6,23–25] Typical examples include N-DMBI-doped N2200, which has a σ of 8×10^{-3} S cm^{-1}, a S of 850 μV K^{-1}, and a resulting PF of 0.6 μW K^{-2} m^{-1}.[15] Recently Pei et al. reported the usage of BDPPV for thermoelectric applications by doping with N-DMBI, which exhibited a σ of 14 S cm^{-1} and PF up to 28 μW K^{-2} m^{-1}.[25] Zhu and his colleagues have spent a lot of efforts on developing n-type thermoelectric materials,[23,24,26] and they have reported, by far, the highest PF values of organic thermoelectric materials, namely the N-DMBI-doped small molecule Q-DCM-DPPTT, which has a σ of 4–5 S cm^{-1}, a S of 660 μV K^{-1} and a PF of over 200 μW K^{-2} m^{-1}.

Even though great progress has been made in the development of OTEs, there are still a lot of important issues remaining to be addressed or to be further investigated. First, it is noted that only a few typical organic semiconductors, such as the p-type ones P3HT and PBTTT, have been intensively studied for thermoelectric applications. However, it is very worthwhile spending more effort on other organic semiconductors, especially given that a handful of D–A copolymer semiconductors, which have the record mobility for polymer semiconductors, have been developed in the last few years.[27–30] It is reported that the maximum ZT achievable in a material is bounded by an intrinsic parameter named transport coefficient (σ_{E_0}), which is a conductivity essential to the charge transport model developed by Synder et al.[31] Given that the conductivity of semiconductor is positively correlated with its carrier mobility when the carrier concentration remains the same, semiconductors with intrinsic high mobility are naturally preferred as thermoelectric materials. Second, as well known, doping is indispensable for achieving high thermoelectric performance. By far the most commonly used dopants for p-doping is F_nTCNQ (n = 2, 4), while the most frequently used n-dopant is N-DMBI. These dopants either have a very deep lowest unoccupied molecule orbitals (LUMO) (p-dopants) or a very shallow highest occupied molecule orbitals (HOMO) (n-dopants), and can effectively dope the semiconductors by forming ion-pairs or charge transfer complex.[32] In the past few years, the dopants and doping techniques for organic semiconductors have been progressed tremendously, with novel dopants like Lewis acid (for p-doing) and Lewis base (for n-doping) demonstrating significant doping effects for improving performance in OFETs or OPVs.[33–36] However, these new doping techniques have not been fully implemented for OTE applications, and therefore it is worth exploring novel dopants to further enhance the thermoelectric performance of OTEs.

Within this background, here we report a systematic study on the thermoelectric properties of a typical high-mobility D–A copolymer semiconductor poly[4-(4,4-dihexadecyl-4H-cyclopenta[1,2-b:5,4-b′]dithiophen-2-yl)-alt-[1,2,5] thiadiazolo[3,4-c]pyridine] (PCDTPT, molecule structure in **Figure 1**a) to reveal the potential of D–A copolymers for OTE applications. In conjunction with PCDTPT, an organic salt trityl tetrakis(pentafluorophenyl) borate (TrTPFB, molecule structure in Figure 1b) was employed for doping as it has been reported to p-dope PCDTPT by a simple solution-blending method in our previous works.[37,38] By varying the doping concentrations, the characteristic parameters of thermoelectric materials such as σ, S and κ were investigated in the temperature range of room temperature (RT ≈ 300 K) to 400 K. It is found that the 5 wt% doped semiconductors have the maximum PF of 7 μW K^{-2} m^{-1} with electrical conductivities approaching 4 S cm^{-1} and Seebeck coefficients of ≈150 μV K^{-1}. Compared to the pristine PCDTPT, the PF and relevant ZT values of 5 wt% doped semiconductors are enhanced by at least three orders of magnitude. These experimental results have indicated that high-mobility D–A copolymers are promising for high-performance thermoelectric materials, and that TrTPFB can be an effective p-dopant for OTE applications, thereby demonstrating a new route to the fabrication of high-performance OTEs.

The molecule structures of PCDTPT and TrTPFB are shown in Figures 1a and 1b, respectively. The electrical performance of pristine PCDTPT field-effect transistors (FETs) in a bottom-gate bottom-contact configuration (BGBC) is illustrated in Figure 1c, from which a saturation mobility of 0.45 cm^2 V^{-1} s^{-1} can be

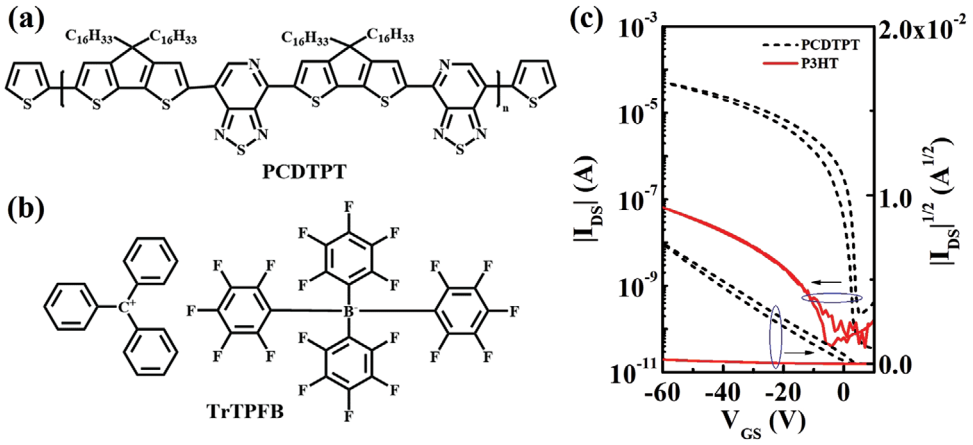

Figure 1. The molecule structures of a) PCDTPT and b) dopant TrTPFB; c) The electrical performance of PCDTPT and P3HT FETs.

obtained. For comparison, we have included the electrical performance of P3HT devices fabricated by the same processing ways, while its mobility is on the order of 10^{-3} cm^2 V^{-1} s^{-1}, almost two orders of magnitude lower than that of PCDTPT. The results indicate that PCDTPT is an intrinsically high-mobility semiconductor and it is supposed to be preferred for thermoelectric applications.

UV-vis-NIR absorption spectrum is often used to identify whether a sample is doped because it is simple and easily available. The pristine PCDTPT was found to have an absorption peak at around 885 nm (**Figure 2**a). It is seen that as the content of TrTPFB increases, the absorption peak gets slightly red-shifted, and the intensity of the main peak is weakened, which may be due to the gradual decrease in the proportion of PCDTPT in the doped samples. Moreover, enhanced absorption in the near infrared region is observed in the doped samples and this absorption gets stronger as the doping concentration increases, suggesting that polarons were formed by the doping.[39] The above features are especially noticeable for the 10 wt% TrTPFB doped samples. To further confirm that PCDTPT was doped by TrTPFB, electron spin resonance (ESR) measurements were performed at room temperature. As seen in Figure 2b, even the 1 wt% TrTPFB doped sample shows strong paramagnetic signals, demonstrating the existence of unpaired electrons.[34] In contrast, PCDTPT and pure TrTPFB (see Figure S2a, Supporting Information) samples were observed without paramagnetic signals. The ESR results further confirm that doping occurs when TrTPFB is blended with PCDTPT. Furthermore, we have also attempted to dope PCDTPT with two other commonly used dopants: F_4TCNQ and $B(C_6F_5)_3$.[20,22,33,40] It turns out that the doping effect of the two dopants are much weaker than that of TrTPFB (see Figures S3 and S4, Supporting Information), indicating TrTPFB is more preferred as the dopant to PCDTPT. All these results justify our choice of the combination of PCDTPT with TrTPFB for thermoelectric studies.

In order to investigate the effect of doping on the surface morphology of PCDTPT films, AFM measurements were carried out and the results are shown in **Figure 3**. It is seen that the surface morphology of the pristine PCDTPT films exhibit very amorphous features, with a small RMS of 0.953 nm. As TrTPFB is introduced into the films, some ordered structures seem to appear. Meanwhile, the RMS values of the doped films are also observed to be generally higher than that of the pristine one (see Figure S5, Supporting Information). The zoomed-in AFM images, which were scanned with a size of 1 × 1 μm, are illustrated in Figure 3d,e,f. To further understand the effect of TrTPFB on film structure of PCDTPT, grazing incidence wide

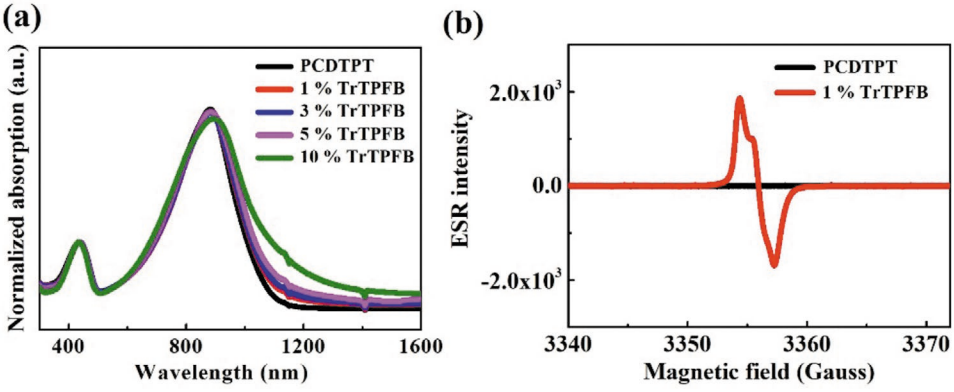

Figure 2. a) The UV-vis-NIR absorption spectra of PCDTPT and doped samples with doping ratio increasing from 1 to 10 wt%; b) ESR spectra of pristine PCDTPT and 1 wt% doped sample.

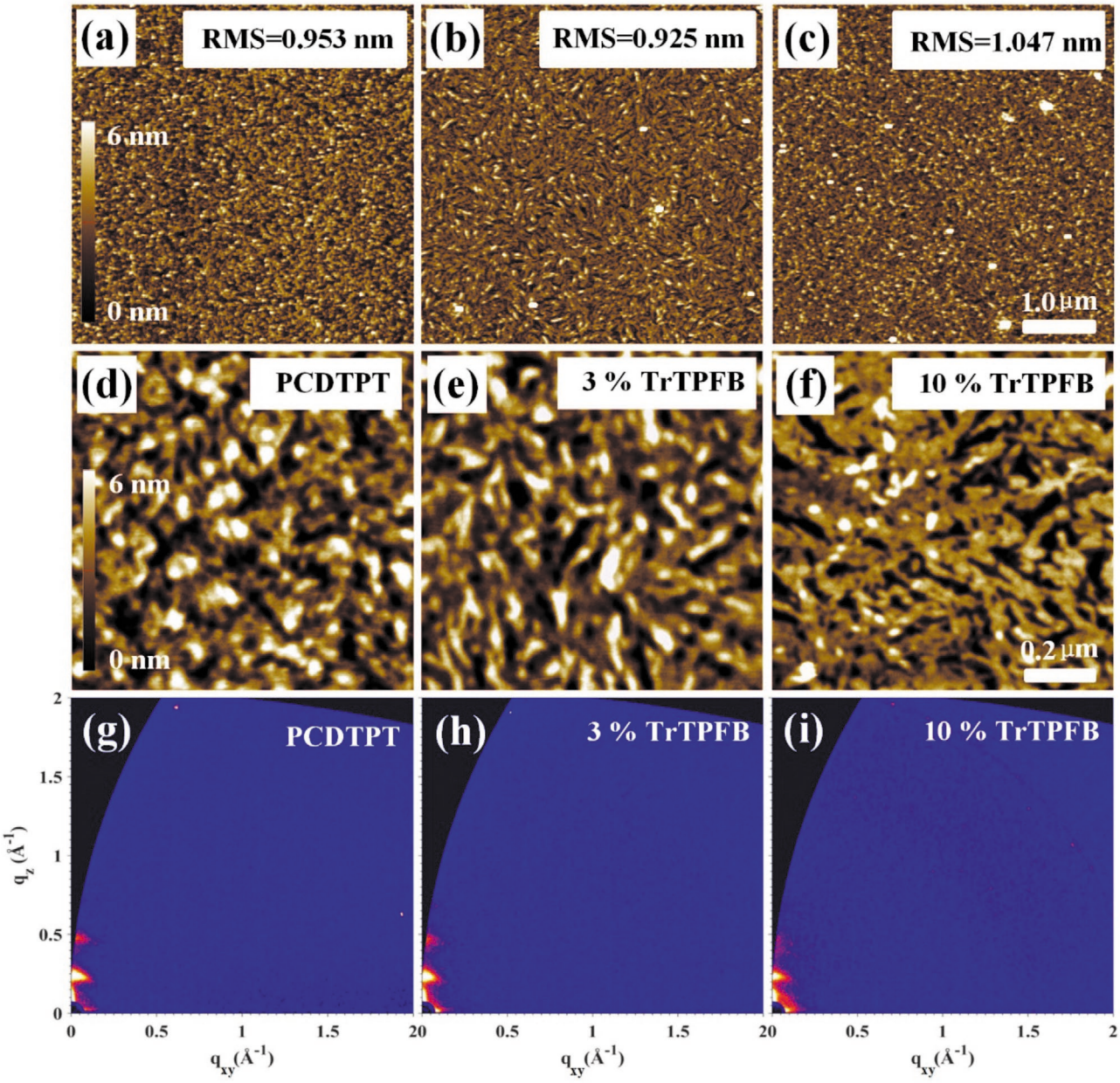

Figure 3. Morphology and structural characterization results. The AFM images of a,d) Pristine PCDTPT; b,e) 3 wt% TrTPFB doped; and c,f) 10 wt% TrTPFB doped PCDTPT films; 2D GIWAXS scattering images of g) Pristine PCDTPT, h) 3 wt% TrTPFB doped, and i) 10 wt% TrTPFB doped PCDTPT films.

angle X-ray scattering (GIWAXS) measurements were performed, with the data shown in Figure 3 g–i. Obvious (100) and (200) lamellar peaks are observed at q_z = 0.240 Å^{-1} and 0.476 Å^{-1} for both the pristine and doped samples, implying the strong edge-on ordering of the polymer molecular packing. In addition, it is seen that the intensity of the peaks gradually decreases as the doping ratio increases (see Figure S6, Supporting Information), indicating the film crystallinity becomes weaker after doping.

To evaluate the thermoelectric properties of the semiconductor materials, we examined the electrical conductivity, Seebeck coefficient and thermal conductivity of the doped films. As shown in **Figure 4**a, though the electrical conductivity of the pristine PCDTPT film is only about 10^{-3} S cm^{-1}, it can be three orders of magnitude enhanced by doping, with a maximum σ of about 4 S cm^{-1} achieved at 400 K for the 10 wt% doped sample. It is seen that σ tends to become saturated when the doping ratio is over 10 wt%. Furthermore, an increasing σ with T was observed, which indicates thermally activated transport behaviors in the materials. By fitting the σ–T data with an Arrhenius equation $\sigma = \sigma_0 \ exp(-\frac{E_A}{kT})$, we can obtain the values of activation energy E_A. Apparently, E_A gets lower as the doping ratio increases, as seen in the plot of the E_A versus σ_{RT} (room

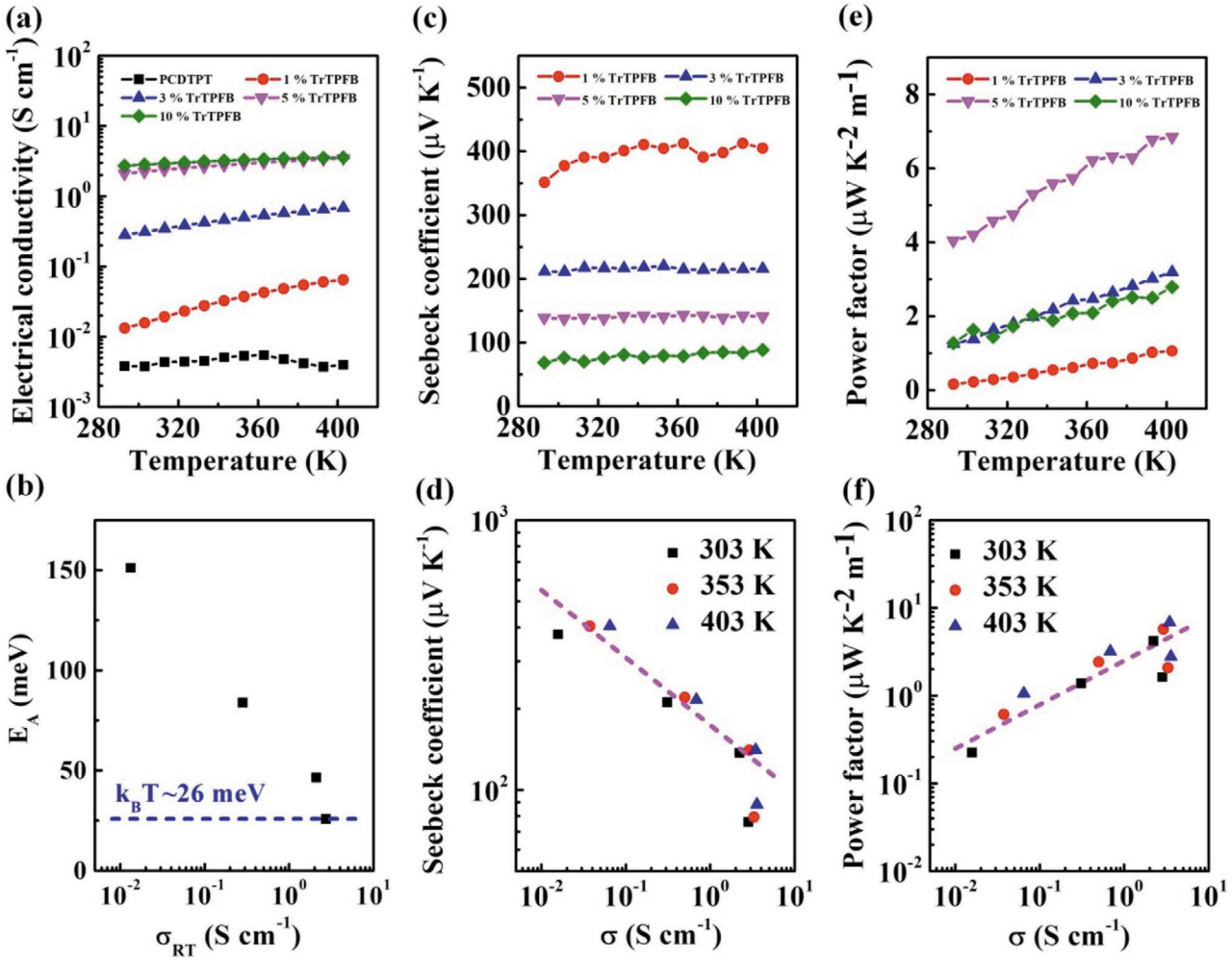

Figure 4. The results of thermoelectric measurements, a) electrical conductivity, c) Seebeck coefficient and e) power factor as a function of temperature for samples with different dopant concentrations; b) Activation energy E_A extracted from the temperature-dependent electrical conductivity shown in (a). The blue dashed line corresponds to the value of $k_BT \approx 26$ meV and σ_{RT} is the room temperature conductivity; d) Seebeck coefficient and f) Power factor at different temperatures as a function of electrical conductivity. The slope of the pink dashed lines in (d) and (f) are −1/4 and 1/2, respectively.

temperature conductivity) in Figure 4b, which is consistent with previous reports.[20] Notably, the E_A values obtained in this work are much lower than those of P3HT: F_4TCNQ and PBTTT: F_4TCNQ reported by Chabinyc at al.,[20] with the lowest E_A extracted from the 10 wt% doped sample comparable to the k_BT limit, (T = 300 K). The low E_A shown in this work is probably resulted from the low activation energy of semiconductor PCDTPT, which was reported to have an E_A of only 40 meV for the field-effect mobility.[38] It is also likely that the dopant TrTPFB contribute to the low E_A in the PCDTPT: TrTPFB system, which remains to be investigated further.

Figure 4c exhibits the Seebeck coefficients of the four doped samples measured at different temperatures. The sign of S is consistent with the fact that holes are majority carriers in the semiconductor. It is noticed that S is almost independent with temperature, which is documented as an indication of hopping transport that is commonly seen in organic semiconductors,[5,24] and this observation is consistent with the thermally activated transport as revealed by the temperature-dependent conductivity measurements mentioned above. Furthermore, we note that S decreases from about 400 μV K^{-1} for the 1 wt% doped sample to 90 μV K^{-1} for the 10 wt% doped one. The decreasing S with increasing dopant concentration has been frequently observed in the doped organic semiconductors. Of particular interest is that the correlation between S and σ in this PCDTPT: TrTPFB system seems to follow the empirical relationship $S \propto \sigma^{-1/4}$ when doping ratio is less than 10 wt%, as indicated by the dash line in Figure 4d.[5,20] The mechanism of such a relationship is still unclear yet. Nevertheless, the consistence of the above results with previous literature reports corroborates the reliability of our measurements.

With the measured electrical conductivities and Seebeck coefficients, the PF for the doped PCDTPT samples can be readily obtained. Figure 4e illustrates the temperature-dependent PF for the samples with four doping ratios. The PF is found to increase with temperatures, which can be ascribed to the thermally activated conductivity. It turns out the 5 wt% doped sample yields the highest PF values, with a maximum

PF approaching 7 μW K^{-2} m^{-1} at 400 K. This is not the highest *PF* for p-doped organic semiconductors, but still among the highest *PF*s for D–A structured copolymer semiconductors.[14,41] In addition, we have plotted the dependence of *PF* on σ, and found that the data is in line with the relationship: $PF \propto \sigma^{1/2}$, as shown in Figure 4f. This is actually a natural result of $S \propto \sigma^{-1/4}$ given that $PF = S^2 \sigma$.

Moreover, we measured the in-plane thermal conductivities of the doped samples for obtaining *ZT* values. The thermal conductivities were found to vary between 0.3–0.4 W K^{-1} m^{-1} for different doping ratios, with a specious trend of increasing thermal conductivity with increasing doping ratios (see Figure S7a, Supporting Information). According to the measured κ, the *ZT* values were obtained instantly, and the highest *ZT* we have achieved is about 0.007 for the 5 wt% doped sample (see Figure S7b, Supporting Information). Note that in our thermoelectric measurement setup, all three characteristic parameters, namely σ, *S*, and κ, were measured on the same sample in the in-plane direction. Therefore, the ZT values presented in this work stand the actual in-plane thermoelectric properties with an error bar around 15%.[43]

In conclusion, we have performed systematic studies of the thermoelectric properties of a high-mobility D–A copolymer semiconductor PCDTPT, which was doped by an organic salt dopant TrTPFB. The combination of UV-vis-NIR spectra and ESR characterizations indicates that the dopant can effectively p-dope the semiconductor, and thus has a dramatic influence on the electrical conductivity and Seebeck coefficient. Temperature-dependent measurements on conductivity, Seebeck coefficient and power factor have yielded in-depth information regarding the thermoelectric performance of the material. The doped PCDTPT is found to adopt hopping transport with very low activation energy. The Seebeck coefficient and power factor in the materials are observed to follow the empirical relationship of: $S \propto \sigma^{-1/4}$ and $PF \propto \sigma^{1/2}$, respectively. A high power factor up to 7 μW K^{-2} m^{-1} for the 5 wt% TrTPFB-doped PCDTPT was obtained, which is among the highest *PF* values for p-type D–A copolymer semiconductors. Moreover, the low in-plane thermal conductivity of about 0.4 W K^{-1} m^{-1} results in an in-plane *ZT* value of 0.007 for that doped sample. It is for the first time that the high-mobility PCDTPT together with TrTPFB are reported for thermoelectric investigations. These results demonstrate that high-mobility D–A copolymer semiconductors represent a promising class of materials for high-performance OTEs. The exploration of novel dopants like TrTPFB also opens up new opportunities for further enhancement of OTE performance.

Experimental Section

Preparation of Doped Samples: TrTPFB (purchased from Strem Chemicals, Inc.) and PCDTPT were dissolved in chlorobenzene (purchased from Sigma–Aldrich, Inc.) to form solutions at concentrations of 5 and 20 g L^{-1}, respectively. Immediately thereafter, different amounts of the two solutions were mixed to obtain solutions of 1, 3, 5, and 10 wt% TrTPFB doped PCDTPT solutions. Then, all the mixed solutions were diluted to a concentration of 10 g L^{-1} for structural characterizations and further thermoelectric property measurements.

Doping Characterizations and Film Morphologies: UV-vis-NIR absorption spectra were measured with UV-3600PLUS (SHIMADZU) in solution samples. To confirm the occurrences of doping in the system, electron spin resonance (ESR) (JES-FA200) measurements were also carried out. The samples were prepared by dropping solutions into paramagnetic tubes and then dried in a glove box. In order to characterize the film morphology, semiconductor solutions were spin coated on SiO_2/Si substrates at 2000 rpm for 30 s, followed by thermal annealing at 150°C for 10 min. Then, atomic force microscopy (AFM) measurements were performed in non-contact mode on a Park XE-7 System.

Fabrication and Characterization of Field-Effect Transistors: Bottom-contact electrodes (Cr/Au: 2 nm/30 nm) were defined by photolithography on Si^{++}/SiO_2 (300 nm) substrates with a channel length of 160 μm and width of 1000 μm. The substrates were cleaned sequentially using deionized water, acetone, and isopropanol, and blown dry by nitrogen gas. Subsequently, the substrates were passivated by trichloro(octadecyl)silane to reduce surface traps. PCDTPT and P3HT films were deposited onto the substrates as described above. The electrical performance of the devices was measured in glove box by an Angilent B2912A source meter.

Electrical Conductivity, Seebeck Coefficient and Thermal Conductivity Measurements: To characterize the thermoelectric properties of our samples, the as-fabricated solutions with various doping ratios were separately transferred onto pre-structured measurement platforms (see Figure S1, Supporting Information)[42,43] via dip-dropping method. First, the platforms were baked on a hot plate at 50 °C for 12 h, and then annealed at 150 °C for 10 min. Finally, the sample was naturally cooled down to room temperature. The film thicknesses of each device were measured by a stylus profilometer (Bruker Dektak) and listed in Table S1, Supporting Information. More fabrication details of the pre-structured platform could be found in ref. [42]. Based on this kind of platform, the full in-plane thermoelectric properties of thin film (σ, *S*, and κ) could be measured.

Supporting Information

Supporting Information is available from the Wiley Online Library or from the author.

Acknowledgements

J.G. and G.L. contributed equally to this work. Y.H. thanks the National Natural Science Foundation of China (61804051) and the Hunan Provincial Talents Program (2018RS053) for financial support. G.L. thanks financial support from the European Union (EU) and the Free State of Saxony through the European Regional Development Fund (ERDF) (SAB GroTEGx, grant no. 100245375) and the support by the startup funding from the Institute of Physics at the Chinese Academy of Sciences.

Conflict of Interest

The authors declare no conflict of interest.

Keywords

doping, organic salts, organic semiconductors, thermoelectric (TE) devices

Received: September 2, 2019
Revised: November 18, 2019
Published online: January 16, 2020

[1] C. Zhou, C. Dun, B. Ge, K. Wang, Z. Shi, G. Liu, D. L. Carroll, G. Qiao, *Nanoscale* **2018**, *10*, 14830.
[2] G. Tan, L. D. Zhao, M. G. Kanatzidis, *Chem. Rev.* **2016**, *116*, 12123.
[3] C. Cho, B. Stevens, J. H. Hsu, R. Bureau, D. A. Hagen, O. Regev, C. Yu, J. C. Grunlan, *Adv. Mater.* **2015**, *27*, 2996.
[4] K. Shi, F. Zhang, C. A. Di, T. W. Yan, Y. Zou, X. Zhou, D. B. Zhu, J. Y. Wang, J. Pei, *J. Am. Chem. Soc.* **2015**, *137*, 6979.
[5] B. Russ, A. Glaudell, J. J. Urban, M. L. Chabinyc, R. A. Segalman, *Nat. Rev. Mater.* **2016**, *1*, 16050.
[6] X. G. Zhao, D. Madan, Y. Cheng, J. W. Zhou, H. Li, S. M. Thon, A. E. Bragg, M. E. DeCoster, P. E. Hopkins, H. E. Katz, *Adv. Mater.* **2017**, *29*, 1606928.
[7] Y. F. Liu, M. H. Zhou, J. He, *Scr. Mater.* **2016**, *111*, 39.
[8] Q. H. Zhang, X. Ai, L. J. Wang, Y. X. Chang, W. Luo, W. Jiang, L. D. Chen, *Adv. Funct. Mater.* **2015**, *25*, 966.
[9] H. J. Wu, B. Y. Chen, H. Y. Cheng, *Acta Mater.* **2017**, *122*, 120.
[10] G. Li, J. G. Fernandez, D. A. L. Ramos, V. Barati, N. Pérez, I. Soldatov, H. Reith, G. Schierning, K. Nielsch, *Nat. Electron.* **2018**, *1*, 555.
[11] X. Li, J. Zhang, Z. Zhao, L. Wang, H. Yang, Q. Chang, N. Jiang, Z. Liu, Z. Bian, W. Liu, *Adv. Mater.* **2018**, *30*, 1705005.
[12] Y. Hu, D. X. Cao, A. T. Lill, L. Jiang, C. A. Di, X. Gao, H. Sirringhaus, T. Q. Nguyen, *Adv. Electron. Mater.* **2018**, *4*, 1800175.
[13] L. Dou, J. You, Z. Hong, Z. Xu, G. Li, R. A. Street, Y. Yang, *Adv. Mater.* **2013**, *25*, 6642.
[14] Y. Chen, Y. Zhao, Z. Liang, *Energy Environ. Sci.* **2015**, *8*, 401.
[15] R. A. Schlitz, F. G. Brunetti, A. M. Glaudell, P. L. Miller, M. A. Brady, C. J. Takacs, C. J. Hawker, M. L. Chabinyc, *Adv. Mater.* **2014**, *26*, 2825.
[16] Q. Zhang, Y. Sun, W. Xu, D. Zhu, *Adv. Mater.* **2014**, *26*, 6829.
[17] D. X. Crispin, *Energy Environ. Sci.* **2012**, *5*, 9345.
[18] G. H. Kim, L. Shao, K. Zhang, K. P. Pipe, *Nat. Mater.* **2013**, *12*, 719.
[19] Q. Zhang, Y. Sun, W. Xu, D. Zhu, *Macromolecules* **2014**, *47*, 609.
[20] A. M. Glaudell, J. E. Cochran, S. N. Patel, M. L. Chabinyc, *Adv. Energy Mater.* **2015**, *5*, 1401072.
[21] G. Zuo, O. Andersson, H. Abdalla, M. Kemerink, *Appl. Phys. Lett.* **2018**, *112*, 083303.
[22] S. N. Patel, A. M. Glaudell, K. A. Peterson, E. M. Thomas, K. A. O'Hara, E. Lim, M. L. Chabinyc, *Sci. Adv.* **2017**, *3*, e1700434.
[23] D. Huang, C. Wang, Y. Zou, X. Shen, Y. Zang, H. Shen, X. Gao, Y. Yi, W. Xu, C. a. Di, *Angew. Chem., Int. Ed.* **2016**, *55*, 10672.
[24] D. Huang, H. Yao, Y. Cui, Y. Zou, F. Zhang, C. Wang, H. Shen, W. Jin, J. Zhu, Y. Diao, *J. Am. Chem. Soc.* **2017**, *139*, 13013.
[25] K. Shi, F. Zhang, C. A. Di, T.-W. Yan, Y. Zou, X. Zhou, D. Zhu, J.-Y. Wang, J. Pei, *J. Am. Chem. Soc.* **2015**, *137*, 6979.
[26] F. Zhang, Y. Zang, D. Huang, C. A. Di, X. Gao, H. Sirringhaus, D. Zhu, *Adv. Funct. Mater.* **2015**, *25*, 3004.
[27] L. Ying, B. B. Hsu, H. Zhan, G. C. Welch, P. Zalar, L. A. Perez, E. J. Kramer, T.-Q. Nguyen, A. J. Heeger, W.-Y. Wong, *J. Am. Chem. Soc.* **2011**, *133*, 18538.
[28] H. Chen, Y. Guo, G. Yu, Y. Zhao, J. Zhang, D. Gao, H. Liu, Y. Liu, *Adv. Mater.* **2012**, *24*, 4618.
[29] X. Zhang, H. Bronstein, A. J. Kronemeijer, J. Smith, Y. Kim, R. J. Kline, L. J. Richter, T. D. Anthopoulos, H. Sirringhaus, K. Song, *Nat. Commun.* **2013**, *4*, 2238.
[30] Y. Yamashita, F. Hinkel, T. Marszalek, W. Zajaczkowski, W. Pisula, M. Baumgarten, H. Matsui, K. Müllen, J. Takeya, *Chem. Mater.* **2016**, *28*, 420.
[31] S. D. Kang, G. J. Snyder, *Nat. Mater.* **2017**, *16*, 252.
[32] I. Salzmann, G. Heimel, M. Oehzelt, S. Winkler, N. Koch, *Acc. Chem. Res.* **2016**, *49*, 370.
[33] J. Panidi, A. F. Paterson, D. Khim, Z. Fei, Y. Han, L. Tsetseris, G. Vourlias, P. A. Patsalas, M. Heeney, T. D. Anthopoulos, *Adv. Sci.* **2018**, *5*, 1700290.
[34] A. F. Paterson, L. Tsetseris, R. Li, A. Basu, H. Faber, A. H. Emwas, J. Panidi, Z. Fei, M. R. Niazi, D. H. Anjum, *Adv. Mater.* **2019**, *31*, 1900871.
[35] J. Kim, D. Khim, K. J. Baeg, W. T. Park, S. H. Lee, M. Kang, Y. Y. Noh, D.-Y. Kim, *Adv. Funct. Mater.* **2016**, *26*, 7886.
[36] R. Wang, D. Zhang, S. Xie, J. Wang, Z. Zheng, D. Wei, X. Sun, H. Zhou, Y. Zhang, *Nano Energy* **2018**, *51*, 736.
[37] Y. Hu, V. Brus, W. Cao, K. Liao, H. Phan, M. Wang, K. Banerjee, G. C. Bazan, T. Q. Nguyen, *Adv. Mater.* **2017**, *29*, 1606464.
[38] Y. Hu, Z. D. Rengert, C. McDowell, M. J. Ford, M. Wang, A. Karki, A. T. Lill, G. C. Bazan, T.-Q. Nguyen, *ACS Nano* **2018**, *12*, 3938.
[39] C. K. Mai, H. Zhou, Y. Zhang, Z. B. Henson, T. Q. Nguyen, A. J. Heeger, G. C. Bazan, *Angew. Chem., Int. Ed.* **2013**, *52*, 12874.
[40] Y. Han, G. Barnes, Y.-H. Lin, J. Martin, M. Al-Hashimi, S. Y. AlQaradawi, T. D. Anthopoulos, M. Heeney, *Chem. Mater.* **2016**, *28*, 8016.
[41] K. Kang, S. Schott, D. Venkateshvaran, K. Broch, G. Schweicher, D. Harkin, C. Jellett, C. Nielsen, I. McCulloch, H. Sirringhaus, *Mater. Today Phys.* **2019**, *8*, 112.
[42] V. Linseis, F. Völklein, H. Reith, P. Woias, K. Nielsch, *J. Mater. Res.* **2016**, *31*, 3196.
[43] V. Linseis, Z. M. Hassan, H. Reith, J. Garcia, K. Nielsch, H. Baumgart, E. Redel, P. Woias, *Phys. Status Solidi A* **2018**, *215*, 1700930.